INJECTOR CALCULATIONS AT ORSAY

J. Gao

CTF3 Injector Calculations at LAL/Orsay

presented by J. Gao
CERN, 26 Oct. 2000

- PARMELA simulations of the CTF3 injector (initial phase). Y. Thiery, J. Gao, and J. Le Duff
- Preliminary design of a TW buncher for CTF3 (analytical design, Superfish, Urmel, HFSS). P. Avrakhov, J. Gao, and R. Raphael
- Analytical design of the waveguide-cavity coupling system used in TW buncher and the fully beam loaded accelerating structures. J. Gao

The layout of the injector of the initial stage of CTF3

case 1: one prebuncher

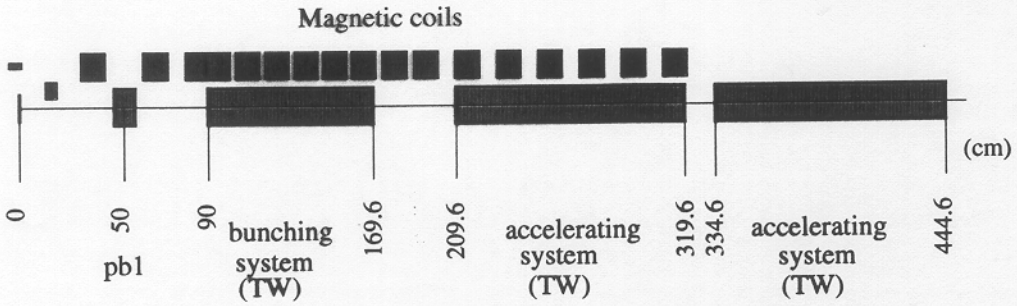

case 2: two prebunchers

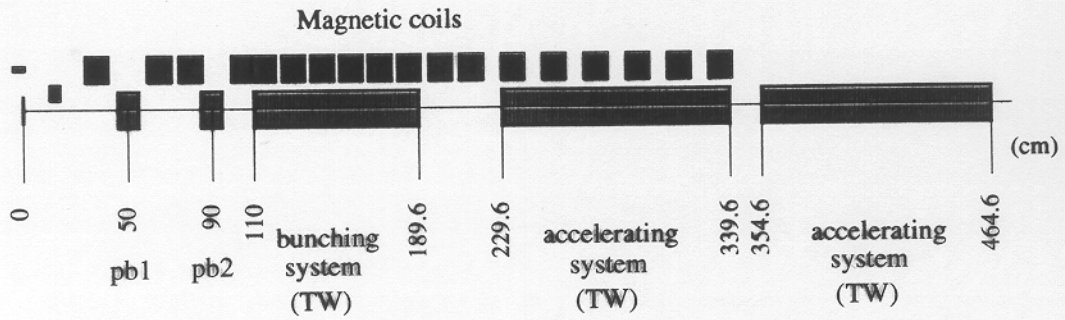

Results of the simulations

(Observation at the end of the second section)

emited particle: 500		phi0±180°		Δphi=20°				
case	Z (cm)'	Nbp	W (MeV)	Nbp	Exrms (mm_mrad)	Eyrms (mm_mrad)	Phirms (deg)	Wrms (MeV)
one prebuncher	444.56	423	22.63	372	37.23	25.99	4.385	0.2362
two prebunchers	464.56	462	22.67	429	23.16	24.04	3.599	0.1679

J. Gao - Y. Thiéry

case 1: one prebuncher

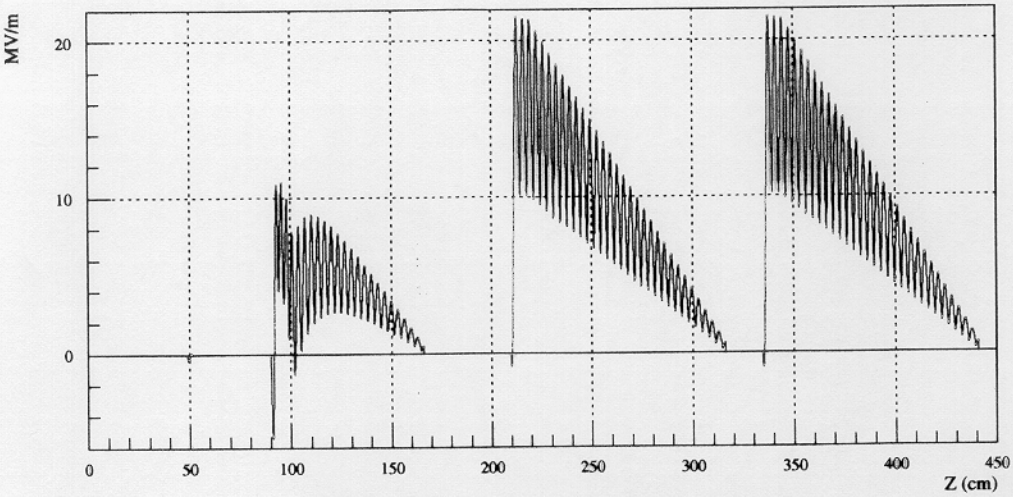

Electric field felt by the reference particle

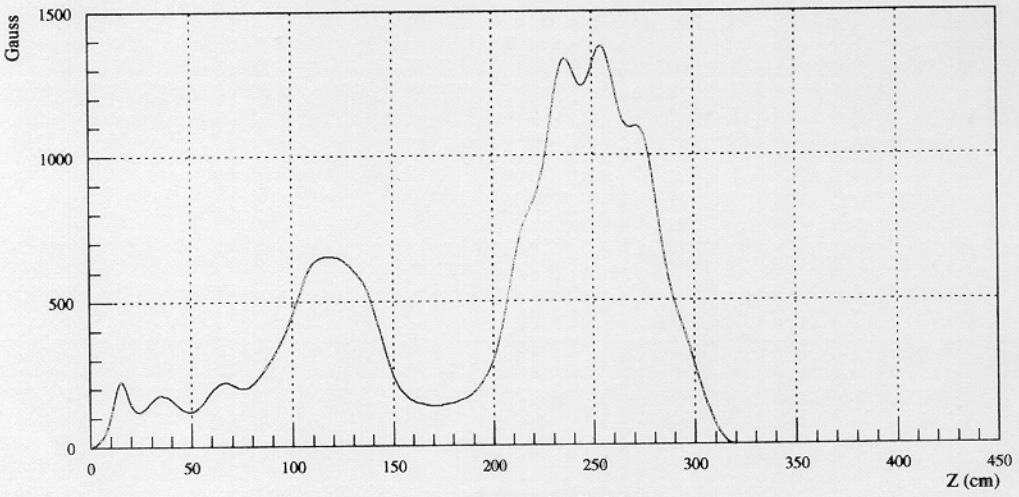

Magnetic field

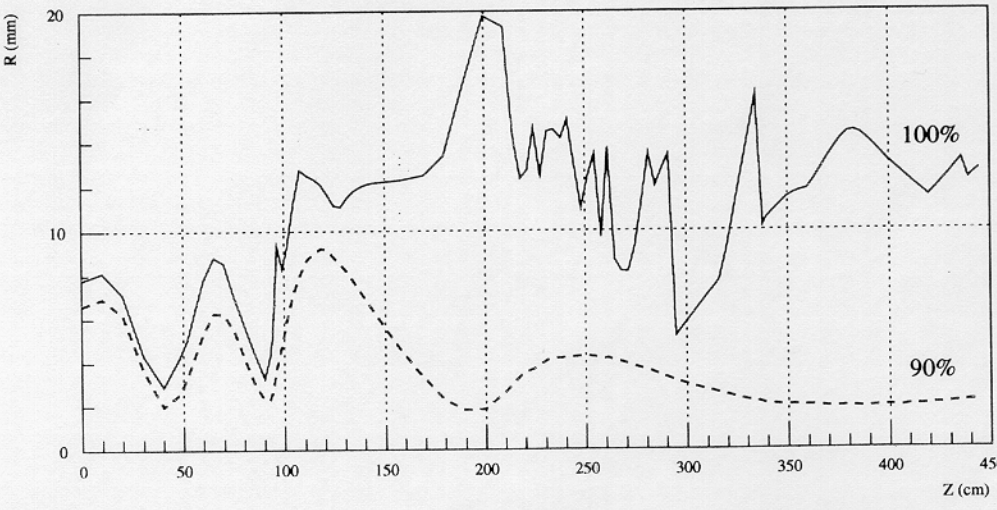

Beam envelope

J. Gao _ Y. Thiéry

case 1: one prebuncher

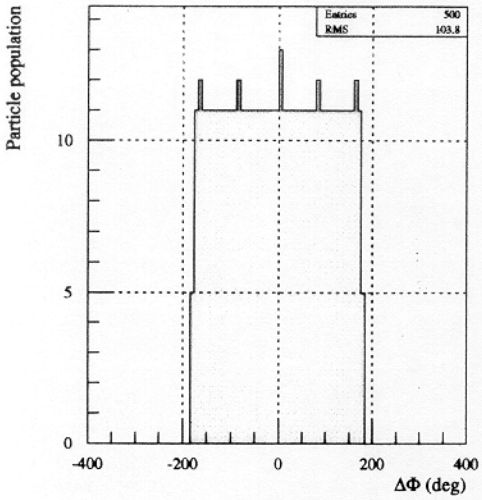

Cathode

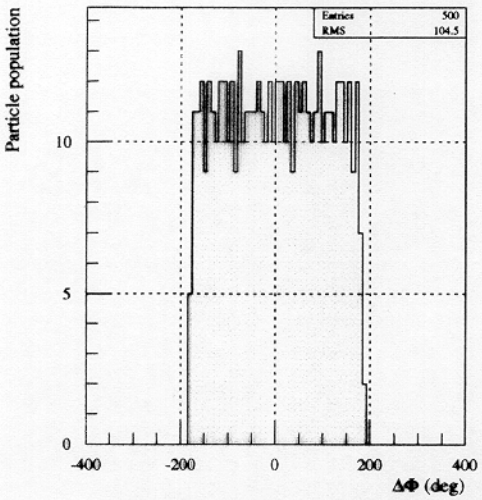

Entrance of the prebuncher

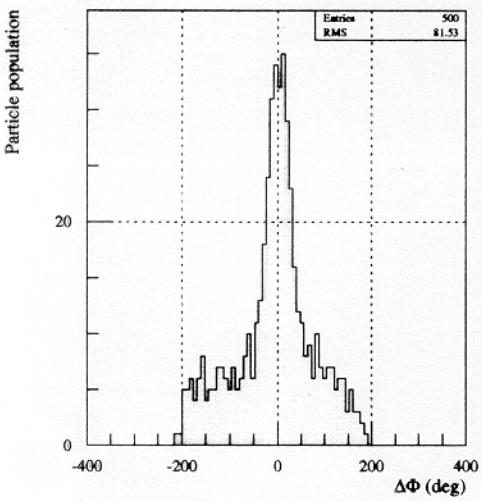

Entrance of the TW buncher

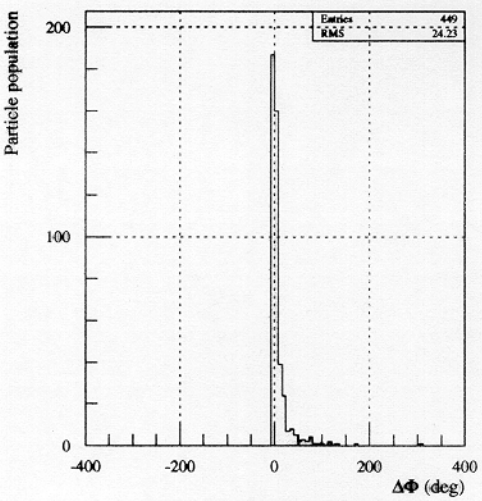

Exit of the TW buncher

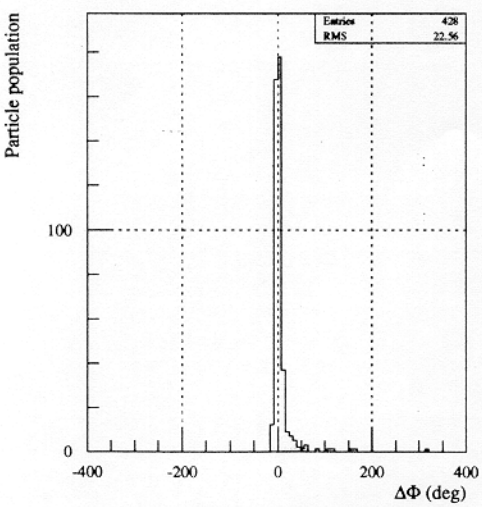

Exit first TW accelerating section

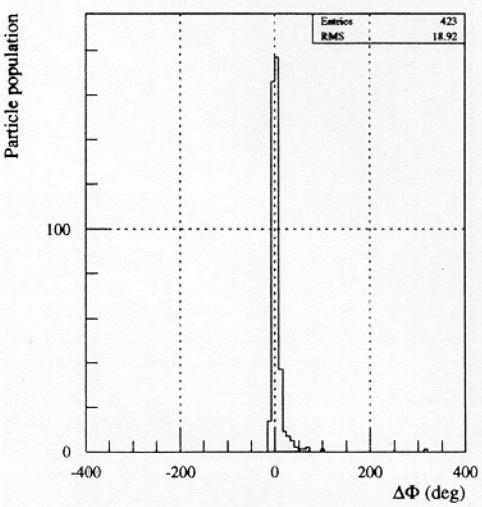

Exit second TW accelerating section

J. Gao - Y. Thiéry

case 1: one prebuncher

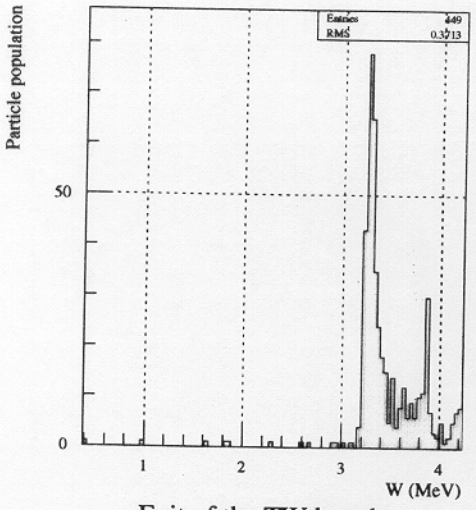

Exit of the TW buncher

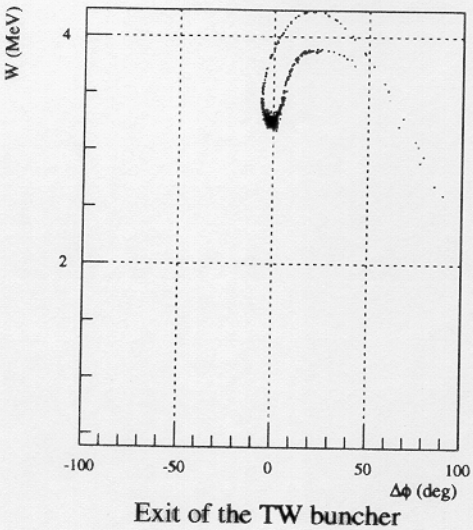

Exit of the TW buncher

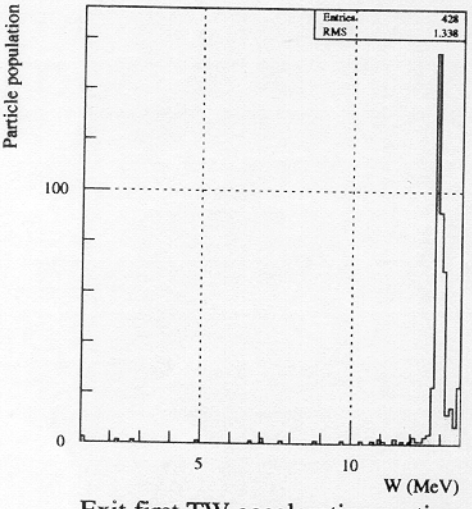

Exit first TW accelerating section

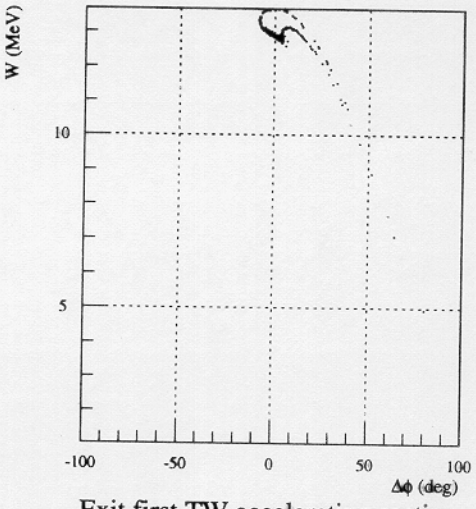

Exit first TW accelerating section

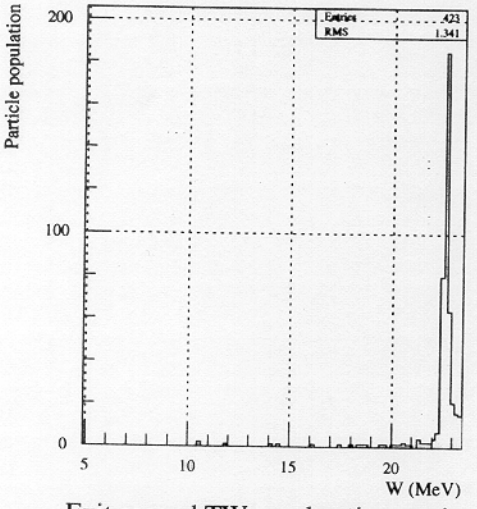

Exit second TW accelerating section

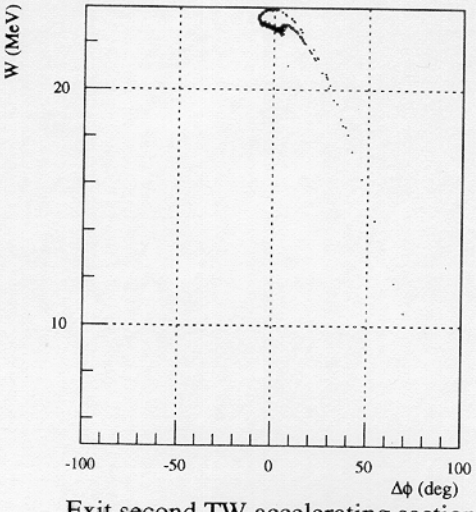

Exit second TW accelerating section

J. Gao _ Y. Thiéry

case 2: two prebunchers

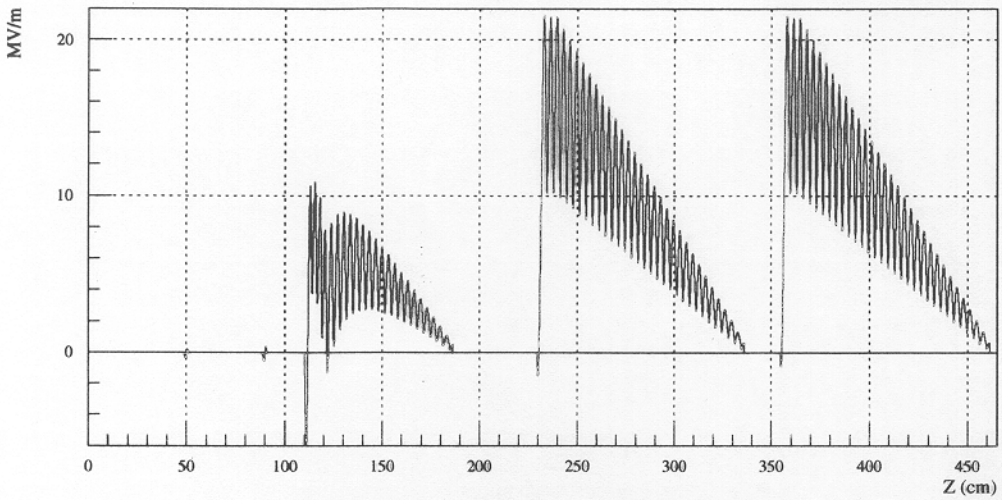

Electric field felt by the reference particle

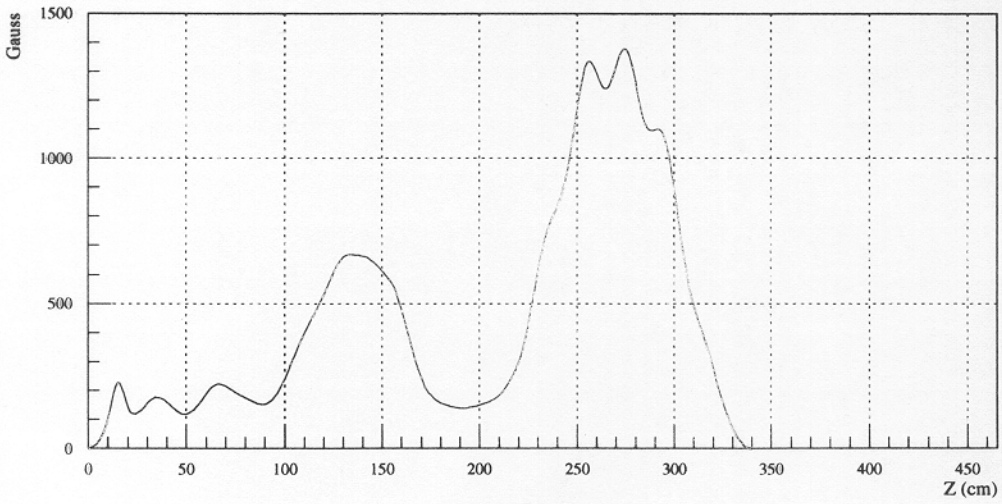

Magnetic field

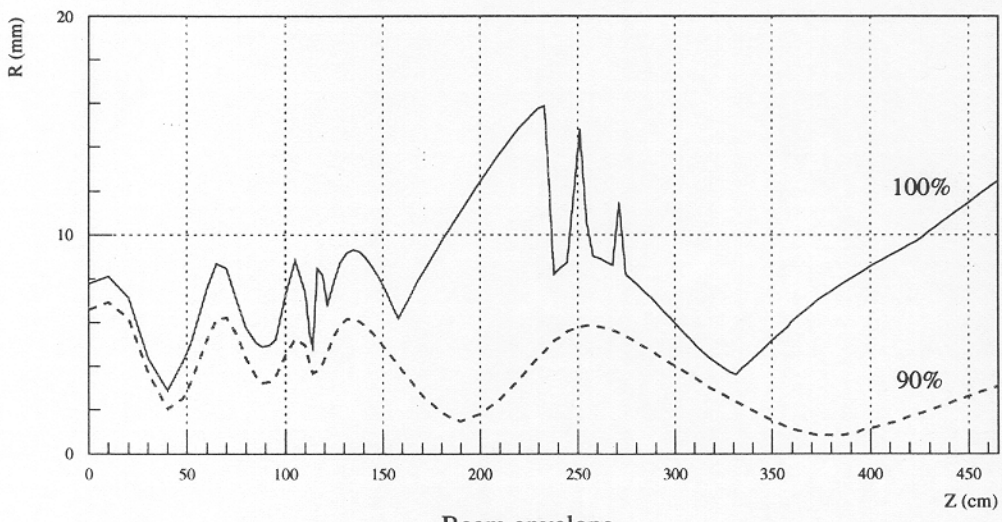

Beam envelope

J. Gao - Y. Thiéry

case 2: two prebunchers

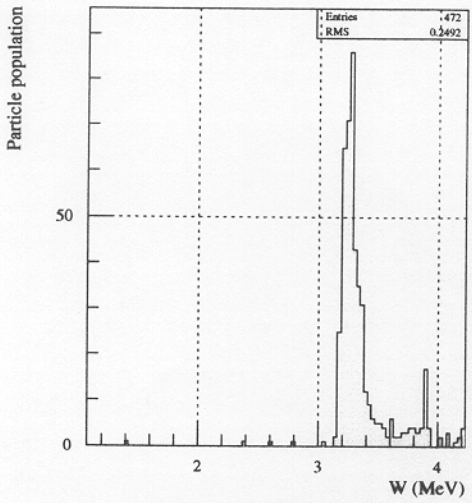

Exit of the TW buncher

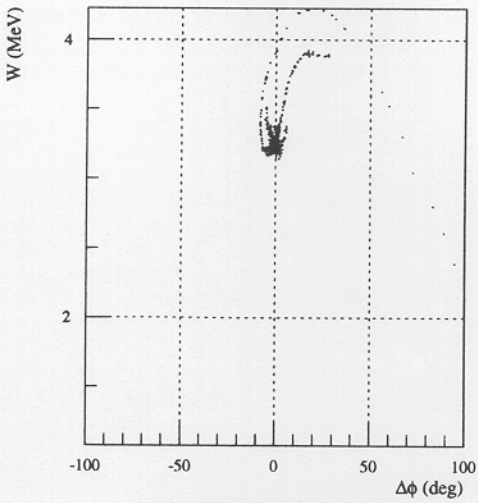

Exit of the TW buncher

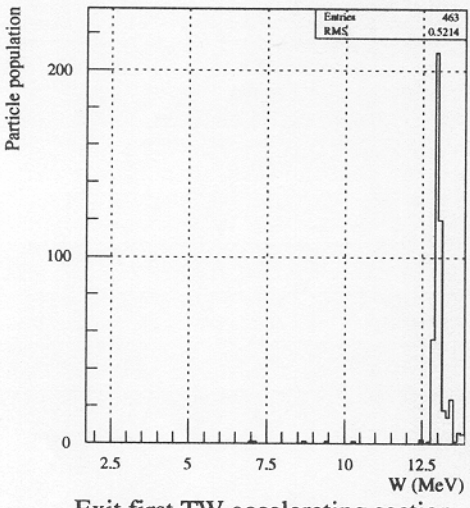

Exit first TW accelerating section

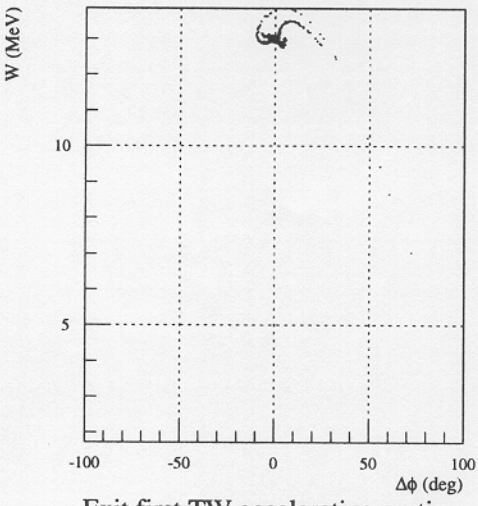

Exit first TW accelerating section

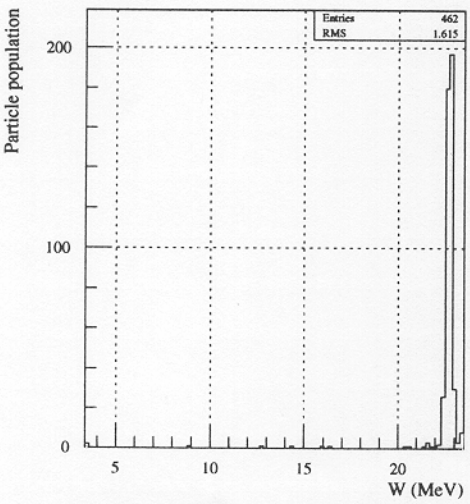

Exit second TW accelerating section

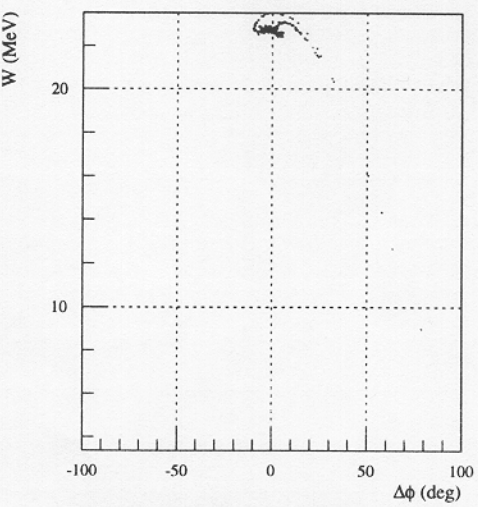

Exit second TW accelerating section

J. Gao - Y. Thiéry

case 2: two prebunchers

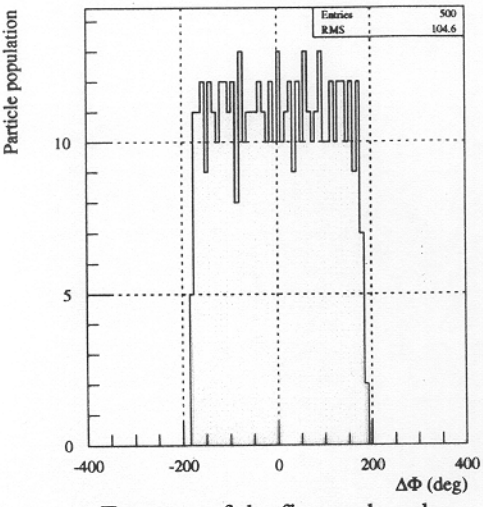

Entrance of the first prebuncher

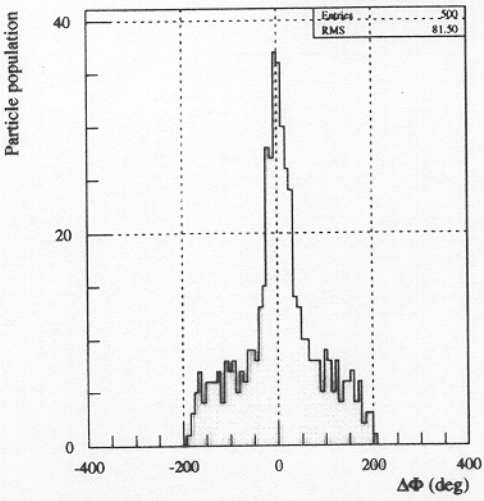

Entrance of the second prebuncher

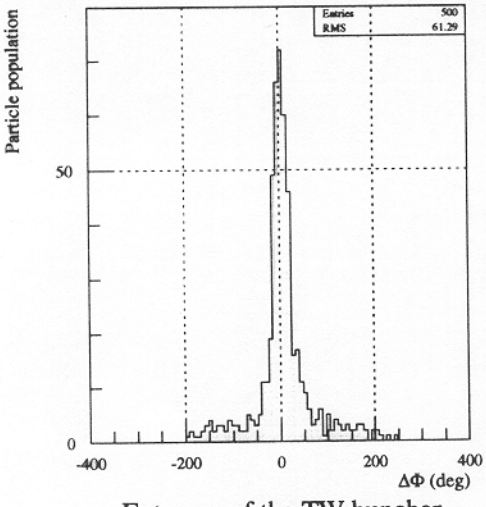

Entrance of the TW buncher

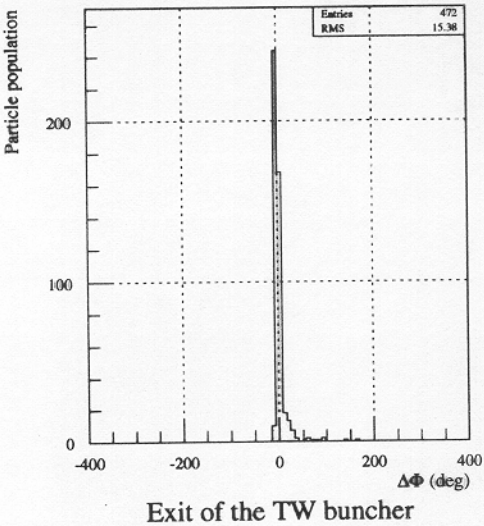

Exit of the TW buncher

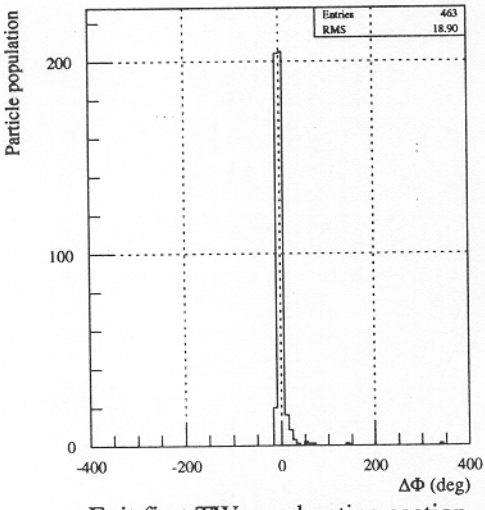

Exit first TW accelerating section

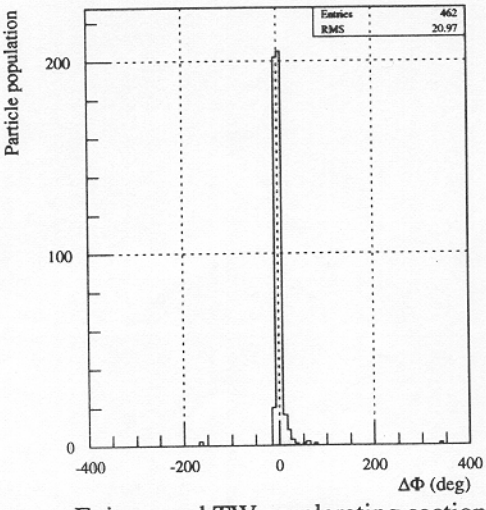

Exit second TW accelerating section

J. Gao - Y. Thiéry

Results of the simulations CTF3

case two prebunchers

(Observation at the end of the second section)

emited particles: 500		phi0±180°		Δphi=20° (±10°)				
W0 (MeV)	Z (cm)	Nbp	W (MeV)	Nbp	Exrms (mm_mrad)	Eyrms (mm_mrad)	Phirms (deg)	Wrms (MeV)
0.135	464.56	430	22.64	358	22.73	21.80	3.454	0.1909
0.140	464.56	462	22.67	429	23.16	24.04	3.599	0.1679
0.145	464.56	466	22.76	383	29.17	27.93	2.510	0.1295

J. Gao - Y. Thiéry

Simulation of TW buncher for CTF3

P. Avrakhov*
LAL, Orsay

Introduction

The simulations results of a high current bunching structure for CLIC [1] Test Facility (CTF3) drive beam are given. The report consists of choosing cavity dimensions and numerical simulations. These results were obtained by using URMEL, SLANS and Ansoft HFSS.

Complex disk-loaded bunching structure

The TW bunching structure for CTF3 [2] drive beam has two kinds of cells with phase velocities β=0.75 and β=1 [3]. The initial part of this cavity has 4 cells with phase velocity 0.75c for frequency 2998 MHz on working mode $2\pi/3$. The second part of the cavity has 24 cells with phase velocity equal the speed of light for the same frequency and working mode.

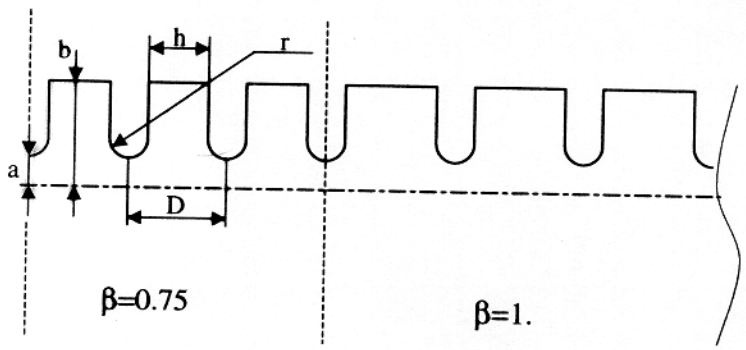

Figure 1. Disk loaded bunching structure with two kind of cells of β=0.75 and β=1.

The initial analytical estimation of the TW buncher cells dimensions is given in Table 1.

Cell type	D (mm)	h (mm)	a (mm)	b (mm)	r(mm)	v_g / c
β=0.75	25	13.7	14.6	40	5.5	0.031
β=1	33	20	16	40	6.6	0.029

Table 1. Preliminary dimensions of the buncher.

In numerical simulations were kept frequency, period D and group velocity v_g of each part of the buncher.

* visitor from BINP, Protvino, Russia

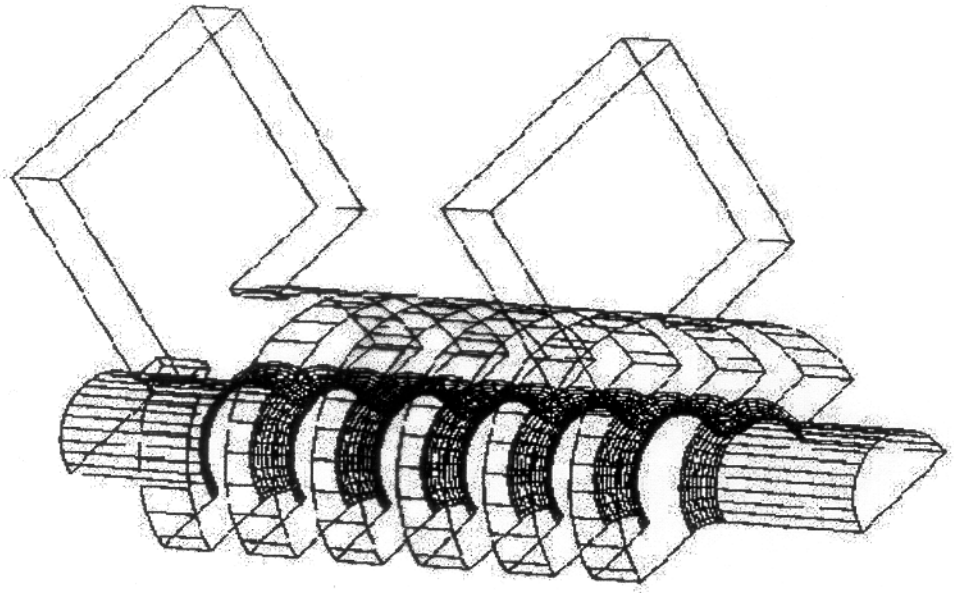

Figure 3. HFSS geometry of a 6-cells model for matching TW buncher coupler cavity.

waveguides. Eigen mode simulations by HFSS shows often big differences with drive solution of the same geometry. A few examples of the drive solutions for this system are given in Figures 6-12.

For the identification of modes real part and phase of electric field on the axis of this model were examined. Figures 4, 5 show the behavior of the electric field and the phase variation for $2\pi/3$ mode. Table 7 and 8 summarize the results for 6-cells model of the first part (β=0.75) and the second part (β=1) of the TW buncher.

Width of coupling slot (mm)	Frequency of $2\pi/3$ mode (MHz)	VSWR on $2\pi/3$ mode frequency
20	2978.8	1.33
30	3008	1.43
35	3005.6	1.02
40	3004.1	1.005

Table 7. HFSS simulation results for the 6-cells model of the first part of the TW buncher with β=0.75

Width of coupling slot (mm)	Frequency of $2\pi/3$ mode (MHz)	VSWR on $2\pi/3$ mode frequency
20	2994.2	1.04
30	2997.7	1.02
40	2992.4	1.007

Table 8. HFSS simulation results for the 6-cells model of the second part of the TW buncher with β=1

Summary of the URMEL simulations

The URMEL simulation for the first part of buncher with β=0.75 is given in Table 2.

Cell type	D (mm)	h (mm)	a (mm)	b (mm)	v_g / c
β=0.75	25.	14.	17.	43.41	0.0312

Table 2. The URMEL simulation results for the first part of the buncher (β=0.75) .

Table 3. shows few points of dispersion curves of the first part of the buncher for fundamental and lowest dipole modes.

Mode	Fundamental	Dipole
0	2889.97	4105.17
π/6	2900.76	4044.71
π/3	2929.07	3964.59
π/2	2965.09	3912.40
2π/3	2998.30	3883.29
5π/6	3020.99	3869.10
π	3028.98	3864.89

Table 3. Points of the lowest dispersion curves for the first part of the buncher (β=0.75) .

Tables 4 and 5 summarize the same parameters for the second part of the buncher with β=1.

Cell type	D (mm)	h (mm)	a (mm)	b (mm)	v_g / c
β=1	33.2	20.	16.8	42.42	0.0295

Table 4. The URMEL simulation results for the second part of the buncher (β=1) .

Mode	Fundamental (MHz)	Dipole (MHz)
0	2923.16	4213.01
π/6	2930.06	4132.75
π/3	2948.61	4060.73
π/2	2973.48	4016.55
2π/3	2997.76	3991.26
5π/6	3015.20	3978.59
π	3021.51	3974.78

Table 5. Points of the lowest dispersion curves for the second part of the buncher (β=1) .

Summary of the HFSS simulations

3-D simulation of the waveguide cavity coupling system of the buncher was produced by using Ansoft HFSS. At first the frequencies of input and output cells are adjusted. It means eigen frequency of the input cell with perfectly loaded waveguide (See Figure 2) equals eigen frequency of intermediate cells of the buncher. The first (phase velocity β=0.75) part and the second (β=1) part of the TW buncher was matched separately.

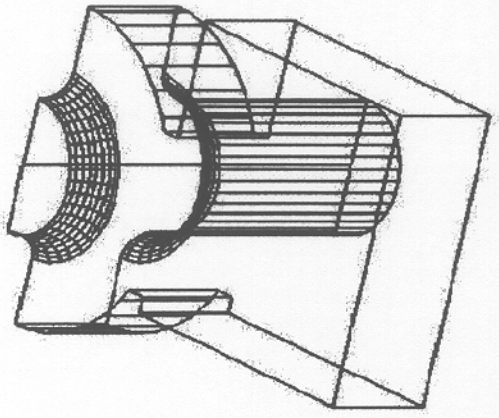

Figure 2. Half of input buncher cell with loaded waveguide

The heights of both waveguides are equal to heights of coupler cells. The distance between axis of the cells and touched inner wall of the waveguide is equal to radius of the coupler cells. Table 6 represents new dimensions of the input cells of the buncher for different width of a coupling slot between the coupler cell and the waveguide.

Coupling slot width (mm)	Radius of input cells (mm) for the part with β=0.75	Radius of input cells (mm) for the part with β=1
20	43.34	42.6
30	-	41.2
35	41.92	-
40	41.08	40.2
50	39.4	-

Table 6. Cell radius of matching input vs coupling slot width.

For the matching of the waveguide coupler to the TW buncher a 6-cells model was used (See Figure 3). The HFSS simulation doesn't provide accurate simulation results in this case. It is explained probably by a high level storage energy on eigen modes in this resonance structure compare with drive energy in

Concluding remarks

For more accurate definition of the coupler dimensions an experimental test or another RF code calculation can be used. In addition the accelerating field distribution in the proposed structure should be computed and adjusted.

Acknowledgments

I thank J. Gao and J. Le Duff for providing useful information and discussions. P. Lepercq and B. Mouton helped me in computer utilization.

References

[1] H. Braun and 10 co-authors, "CLIC – A compact and Efficient High Energy Linear Collider", PAC95, Dallas, May 1995

[2] CLIC study team, "Proposals for future CLIC studies and a new CLIC test facility (CTF3)", CLIC Note 402

[3] Y. Thiery, J. Gao and J. Le Duff, "Design studies for high current bunching system for CLIC test facility (CTF3) drive beam", Note LAL-SERA-2000-130, CERN, May 2-3, 2000

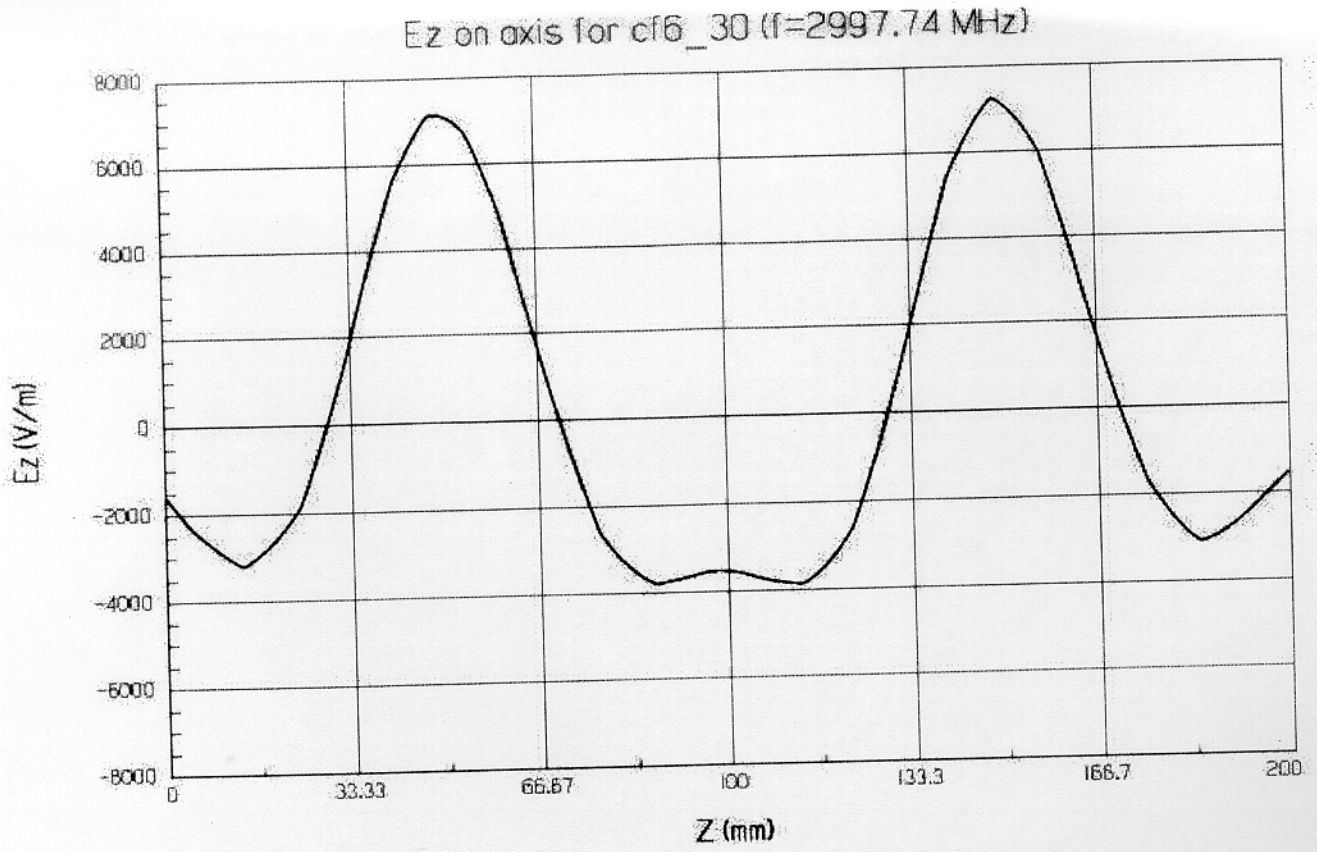

Figure 4. Distribution of Ez on axis for 6-cells model with β=1 (slot=30x20, f=2998 MHz)

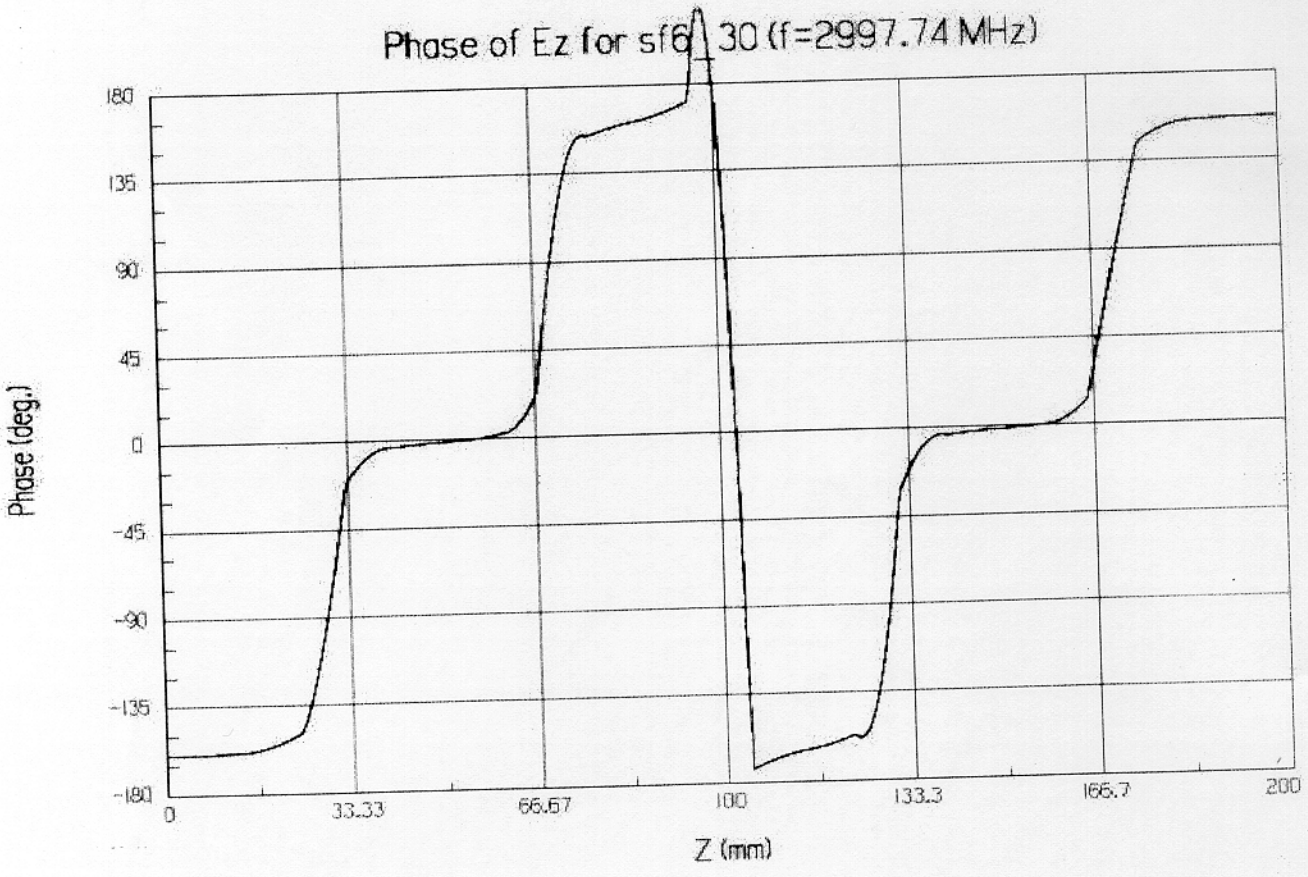

Figure 5. Ez phase distribution on axis for 6-cells model with β=1 (slot=30x20, f=2998 MHz)

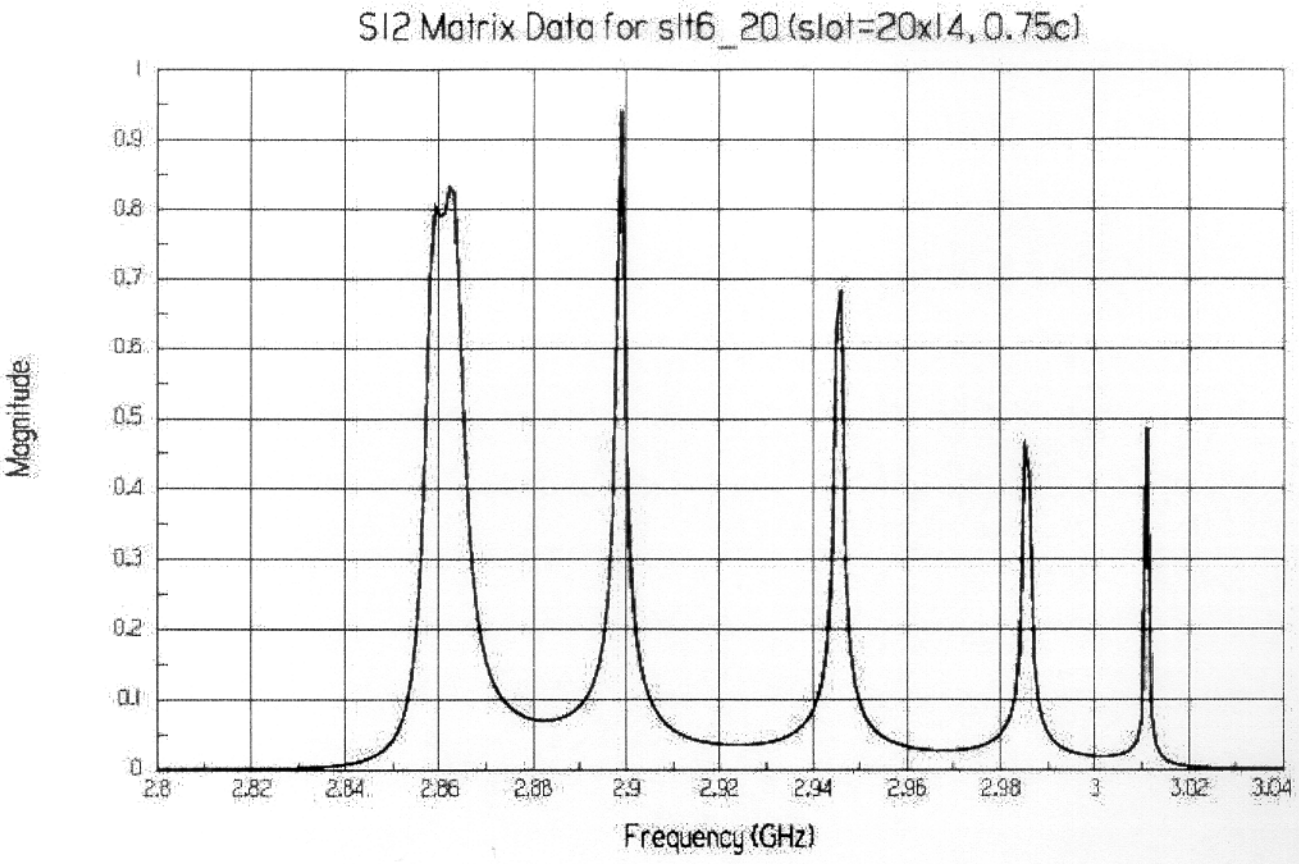

Figure 6. Fundamental mode passband for 6-cells model with β=0.75, slot=20x14

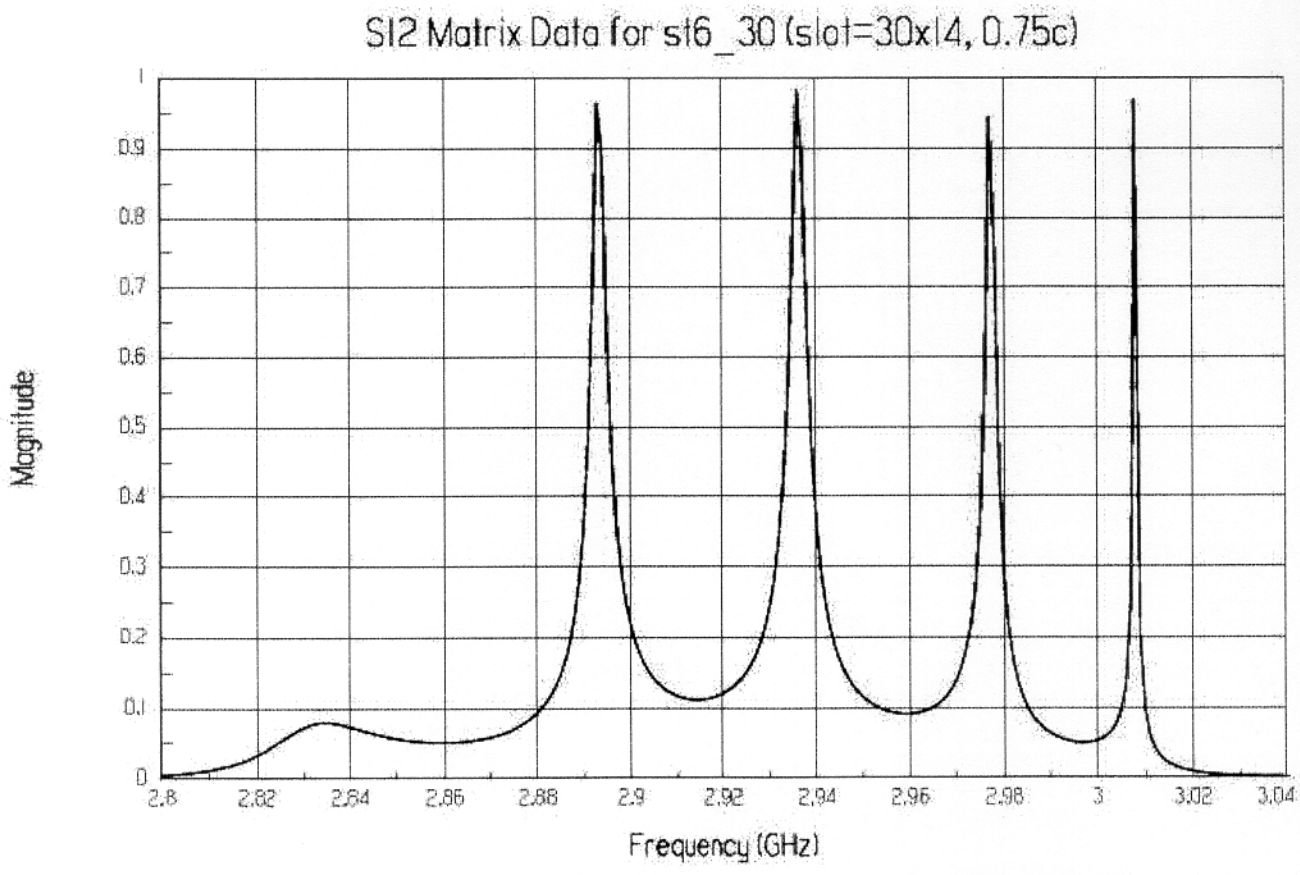

Figure 7. Fundamental mode passband for 6-cells model with β=0.75, slot=30x14

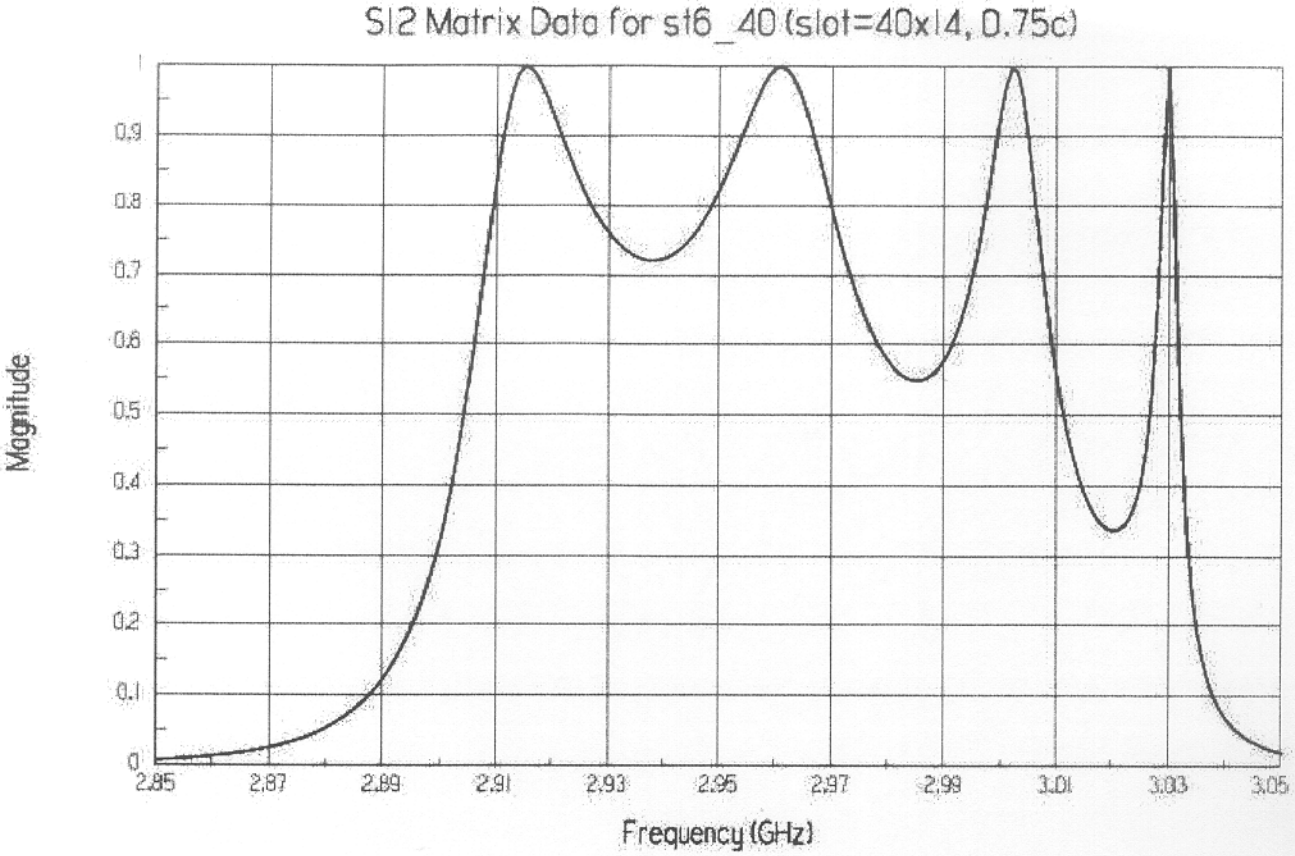

Figure 8. Fundamental mode passband for 6-cells model with β=0.75, slot=40x14

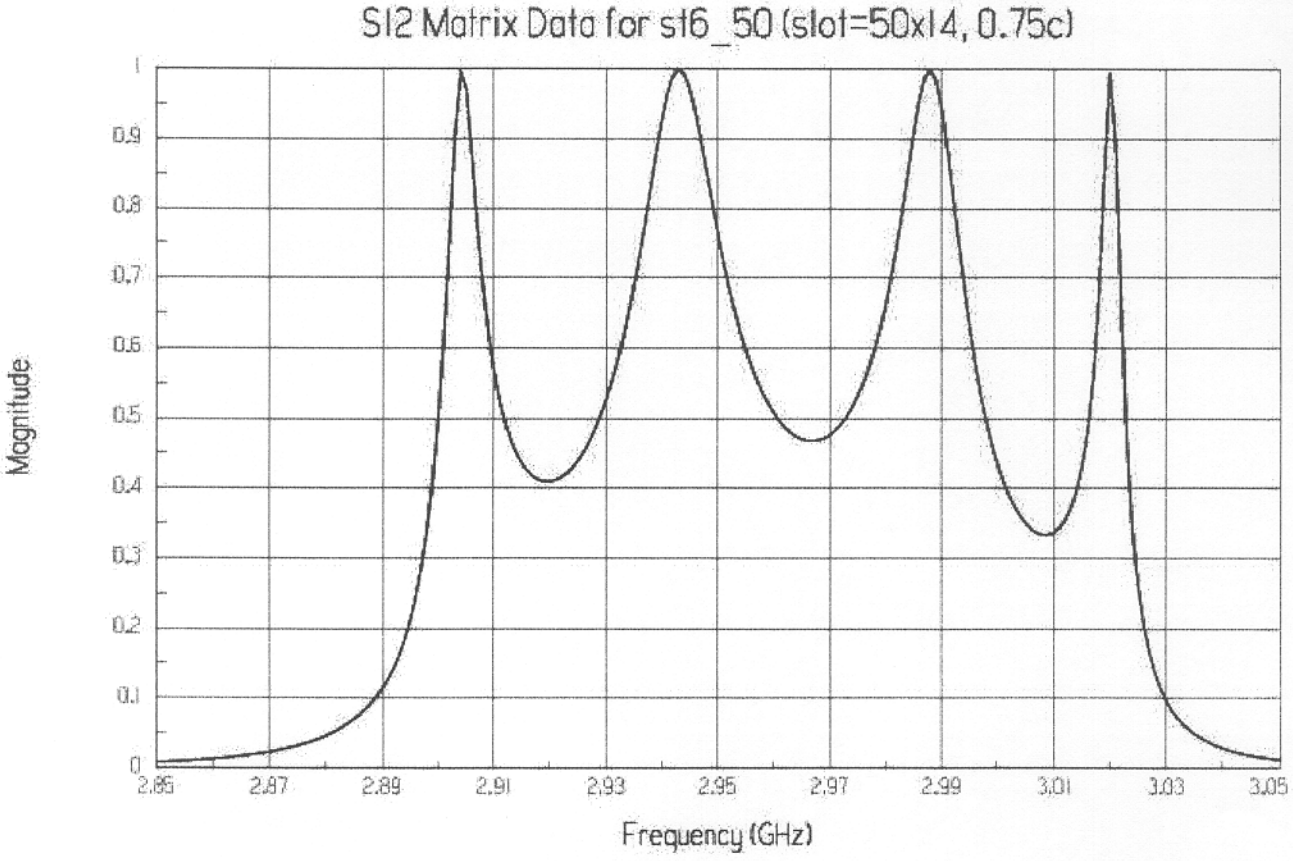

Figure 9. Fundamental mode passband for 6-cells model with β=0.75, slot=50x14

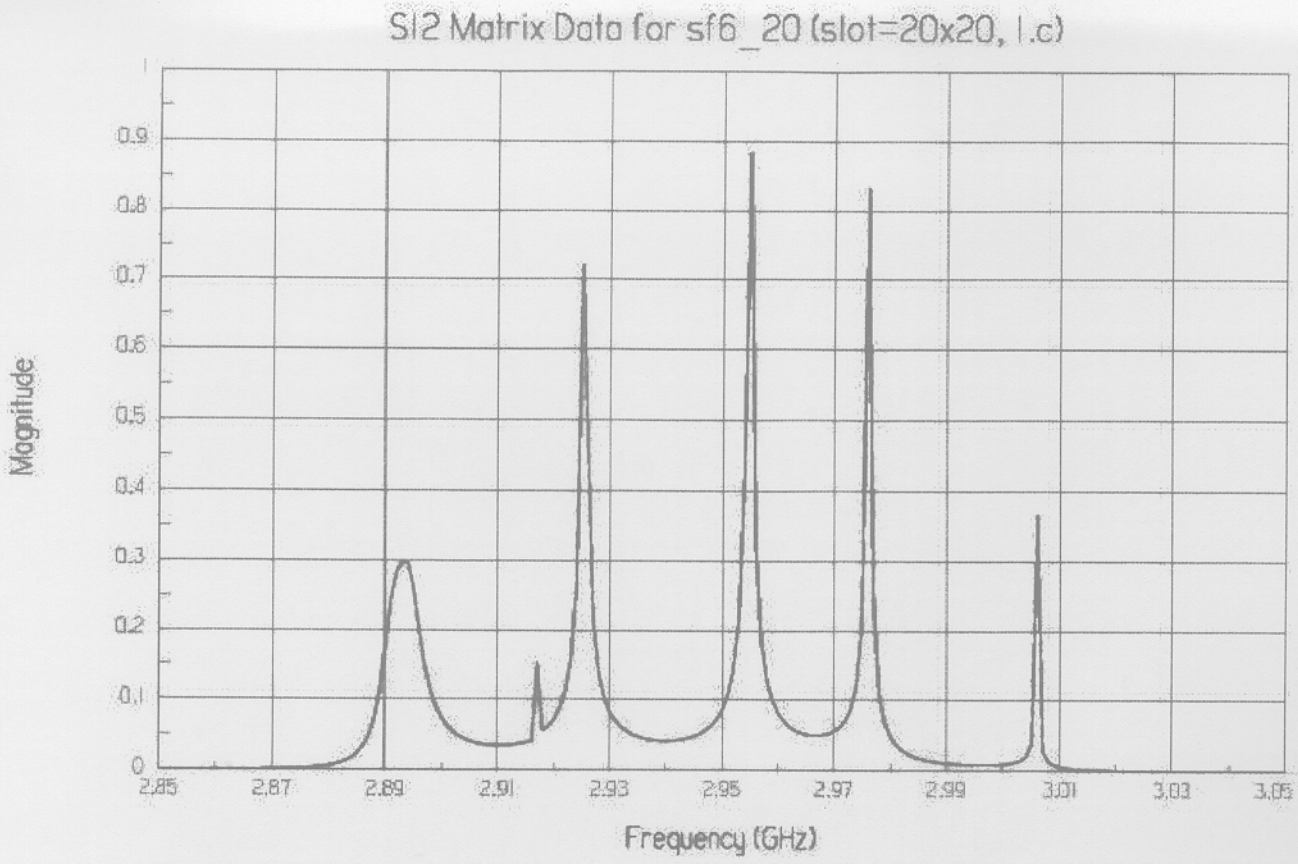

Figure 10. Fundamental mode passband for 6-cells model with β=1, slot=20x20

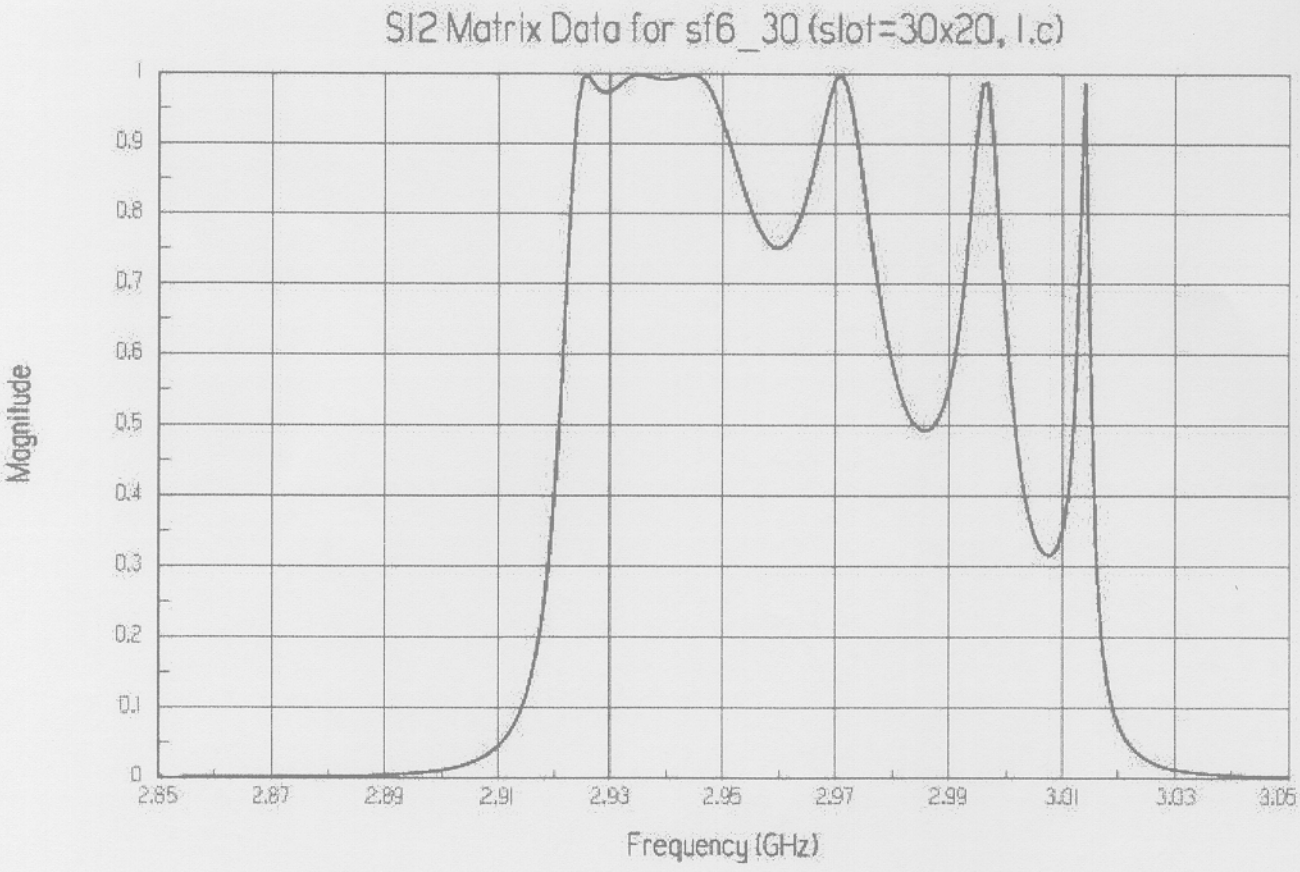

Figure 11. Fundamental mode passband for 6-cells model with β=1, slot=30x20

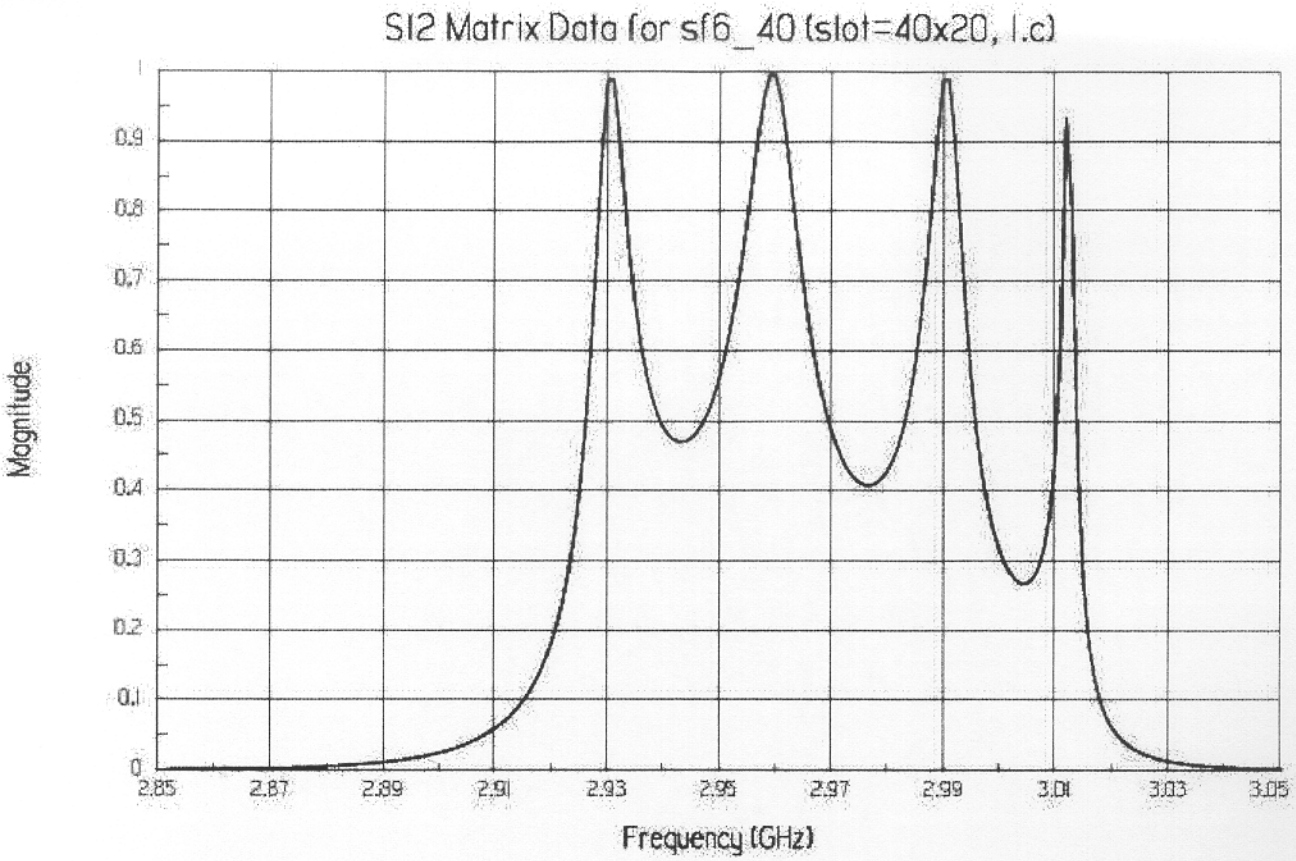

Figure 12. Fundamental mode passband for 6-cells model with β=1, slot=40x20

Analytical Determination of the Coupling Coefficient of a Waveguide Cavity Coupling System

J. Gao
Laboratoire de L'Accélérateur Linéaire
IN2P3-CNRS et Université de Paris-Sud
B.P. 34, 91898 Orsay cedex, France

Abstract

By applying the perturbation method, we show in a general way how to determine the coupling coefficient of a waveguide cavity coupling system and as a special example we derive the analytical expressions of the coupling coefficient for a waveguide-cavity coupling system as shown in Fig. 1. The term "cavity" in this paper stands for the cavity in both standing wave and traveling wave structures.

1 Introduction

In the design and construction of klystrons and linear accelerating structures the coupling systems shown in Fig. 1 [1][2] and Fig. 2 are the most frequently used ones. The cavities can be standing wave or traveling wave ones. To determine the coupling coefficient between the waveguide and the cavity one can use different methods such as experiments, numerical simulations, and analytical calculations. In this paper we will concentrate on the coupling system shown in Fig. 1. The analytical treatment for the coupling system shown in Fig. 2 has been given in refs. [3] and [4].

2 General theory

In a rectangular waveguide of width a and height b the normalized H_{nm} modes can be derived from the scalar function [5]:

$$\psi_{nm}(x,y) = \left(\frac{\epsilon_{0n}\epsilon_{0m}}{abjk_0Z_0\Gamma_{nm}k_{c,nm}^2}\right)^{1/2} \cos\left(\frac{n\pi}{a}\right)\cos\left(m\pi\frac{2y-b}{b}\right) \quad (1)$$

according to the following relations:

$$\mathbf{h}_{znm} = \mathbf{a}_z k_{c,nm}^2 \psi_{nm} \quad (2)$$

$$\mathbf{h}_{nm} = -\Gamma_{nm}\nabla_t\psi_{nm} \quad (3)$$

$$\mathbf{e}_{nm} = \frac{jk_0Z_0}{\Gamma_{nm}}(\mathbf{a}_x\mathbf{a}_y - \mathbf{a}_y\mathbf{a}_x)\cdot\mathbf{h}_{nm} \quad (4)$$

$$\mathbf{E}_{nm}^{\pm} = \mathbf{e}_{nm}e^{\mp\Gamma_{nm}z}\cdot\mathbf{h}_{nm} \quad (5)$$

$$\mathbf{H}_{nm}^{\pm} = (\pm\mathbf{h}_{nm} + \mathbf{h}_{znm})e^{\mp\Gamma_{nm}z} \quad (6)$$

where $\epsilon_{0n} = 1(n=0)$ and $\epsilon_{0n} = 2(n>0)$, $Z_0 = 120\pi(\Omega)$, $k_{c,nm}^2 = (m\pi/b)^2 + (n\pi/a)^2 - k_0^2$, $\mathbf{h}_{nm}$ and $\mathbf{e}_{nm}$ are the transverse magnetic and electric normal mode fields, $\Gamma_{nm}^2 = k_{c,nm}^2 - k_0^2$, $k_0 = 2\pi/\lambda$, and the λ is the wavelength in free space. The normalization in eq. 1 has been chosen so that

$$\int_0^a\int_0^b \mathbf{e}_{nm}\times\mathbf{h}_{nm}\cdot\mathbf{a}_z dxdy = 1 \quad (7)$$

Now we consider the case (see Fig. 3) of a waveguide excited by an aperture (see Fig. 4) which can be equivalent to an electric dipole $\mathbf{P}$ and a magnetic dipole $\mathbf{M}$. The scattered field can be expanded in terms of the normal waveguide modes as follows [5]:

$$\mathbf{E}_s = \sum a_n\mathbf{E}_n^+ \qquad z>0 \quad (8)$$

$$\mathbf{H}_s = \sum a_n\mathbf{H}_n^+ \qquad z>0 \quad (9)$$

$$\mathbf{E}_s = \sum b_n\mathbf{E}_n^- \qquad z<0 \quad (10)$$

$$\mathbf{H}_s = \sum b_n\mathbf{H}_n^- \qquad z<0 \quad (11)$$

where the expansion coefficients a_n and b_n can be obtained by the following relations [5]:

$$2a_n = j\omega(\mu_0 \mathbf{H}_n^- \cdot \mathbf{M} - \mathbf{E}_n^- \cdot \mathbf{P}) \tag{12}$$

$$2b_n = j\omega(\mu_0 \mathbf{H}_n^+ \cdot \mathbf{M} - \mathbf{E}_n^+ \cdot \mathbf{P}) \tag{13}$$

where $\omega = \frac{k_{10}}{c}$, the electric and magnetic dipoles can be estimated as follows [5]:

$$\mathbf{P} = -\frac{\pi l_1^3(1-e_0^2)}{3E_0(e_0)}\epsilon_0 \mathbf{E}_0 \tag{14}$$

$$\mathbf{M}_1 = \frac{\pi l_1^3 e_0^2}{3(K(e_0) - E_0(e_0))}\mu_0 \mathbf{H}_1 \tag{15}$$

$$\mathbf{M}_2 = -\frac{\pi l_1^3 e_0^2(1-e_0^2)}{3(E_0(e_0) - (1-e_0^2)K(e_0))}\mu_0 \mathbf{H}_2 \tag{16}$$

$$K(e_0) = \frac{\pi}{2}\left(1 + \left(\frac{1}{2}\right)^2 e_0^2 + \left(\frac{1\cdot 3}{2\cdot 4}\right)^2 e_0^4 + \left(\frac{1\cdot 3\cdot 5}{2\cdot 4\cdot 6}\right)^2 e_0^6 + \cdots\right) \tag{17}$$

$$E(e_0) = \frac{\pi}{2}\left(1 - \left(\frac{1}{2}\right)^2 e_0^2 - \left(\frac{1\cdot 3}{2\cdot 4}\right)^2 \frac{e_0^4}{3} - \left(\frac{1\cdot 3\cdot 5}{2\cdot 4\cdot 6}\right)^2 \frac{e_0^6}{5} - \cdots\right) \tag{18}$$

$$e_0 = \left(1 - \frac{l_2^2}{l_1^2}\right)^{1/2} \tag{19}$$

where ϵ_0 is the permittivity of the vacuum, and μ_0 is the permeability of the vacuum. When the aperture is circular of radius r, eqs. 14 and 15 can be simplified as follows:

$$\mathbf{P} = -\frac{2}{3}r^3\epsilon_0 \mathbf{E}_0 \tag{20}$$

$$\mathbf{M}_{1,2} = \frac{4}{3}r^3\mu_0 \mathbf{H}_{1,2} \tag{21}$$

As a special example we consider the H_{10} mode in the waveguide. The normalized mode functions for the H_{10} mode are:

$$\mathbf{E}_{10}^+ = \mathbf{e}_{10}e^{-\Gamma_{10}z} \tag{22}$$

$$\mathbf{E}_{10}^- = \mathbf{e}_{10}e^{\Gamma_{10}z} \tag{23}$$

$$\mathbf{H}_{10}^+ = (\mathbf{h}_{10} + \mathbf{h}_{z10})e^{-\Gamma_{10}z} \tag{24}$$

$$\mathbf{H}_{10}^{-} = (-\mathbf{h}_{10} + \mathbf{h}_{z10})e^{\Gamma_{10}z} \tag{25}$$

$$\mathbf{e}_{10} = -jk_0Z_0\left(\frac{2}{jabk_0Z_0\Gamma_{10}}\right)^{1/2}\sin\left(\frac{\pi x}{a}\right)\mathbf{a}_y \tag{26}$$

$$\mathbf{h}_{10} = \Gamma_{10}\left(\frac{2}{jabk_0Z_0\Gamma_{10}}\right)^{1/2}\sin\left(\frac{\pi x}{a}\right)\mathbf{a}_x \tag{27}$$

$$\mathbf{h}_{z10} = \left(\frac{2}{jabk_0Z_0\Gamma_{10}}\right)^{1/2}\frac{\pi}{a}\cos\left(\frac{\pi x}{a}\right)\mathbf{a}_z \tag{28}$$

$$\Gamma_{10} = k_0\left(1 - \left(\frac{\lambda}{2a}\right)^2\right)^{1/2} \tag{29}$$

The peak power of the H_{10} mode inside the waveguide can be expressed as:

$$P_{max} = \frac{abZ_0k_0}{4\Gamma_{10}}H_{x,10,max}^2 \tag{30}$$

$$H_{x,10,max} = \frac{a\Gamma_{10}}{\pi}H_{z,10,max} \tag{31}$$

where $H_{x,10,max}$ and $H_{z,10,max}$ are the peak magnetic fields of the H_{10} mode in the x and z directions, respectively. If on the surface of the dipole there is only magnetic field, the expansion coefficients a_1 and b_1 corresponding to H_{10} mode can be found from eqs. 12 and 13 as follows:

$$2a_1 = j\omega\mu_0\mathbf{H}_{10}^{-}\cdot\mathbf{M} = j\omega\mu_0\mathbf{h}_{z10}\cdot\mathbf{M} \tag{32}$$

$$2b_1 = j\omega\mu_0\mathbf{H}_{10}^{+}\cdot\mathbf{M} = j\omega\mu_0\mathbf{h}_{z10}\cdot\mathbf{M} = 2a_1 \tag{33}$$

With the above preparation one can start to establish the analytical formulae of the coupling coefficient of the waveguide-cavity coupling system shown in Fig. 1. According to the definition one has

$$\beta = \frac{P}{P_0^*} \tag{34}$$

where P is the power radiated into the waveguide from the cavity through the coupling aperture, $P_0^* = P_0 + Uv_g/h$, P_0 is the power dissipated on the coupler cavity wall, U is the energy stored inside the coupler cavity, and

v_g is the group velocity of the structure (the case of $v_g = 0$ corresponds to standing wave cavity). By using eqs. 30 and 34 one finds:

$$\beta = \frac{\pi^2 N Z_0 k_0 \Gamma_{10} e_0^4 l_1^6 e^{-2\alpha d} \sin^2\left(\frac{2\pi L}{\lambda_g}\right)}{9ab(K(e_0) - E(e_0))^2} \left(\frac{\pi}{a\Gamma_{10}}\right)^2 \frac{H_1^2}{P_0^*} \tag{35}$$

where N is the number of the waveguides connected to the coupler cavity (assuming that the magnetic field on each coupling aperture is the same), H_1 is magnetic field at the location of the coupling aperture before the aperture is opened, λ_g is the waveguide wavelength of the H_{10} mode, d is the average wall thickness between the inner surface of the waveguide and the inner surface of the coupler cavity, and α is the attenuation coefficient which can be expressed as $\alpha = \frac{2\pi}{\lambda}((\frac{\lambda}{4l_{1,2}})^2 - 1)^{1/2}$ depending on the wave inside the aperture is H_{10} or H_{01} like. In fact eq. 35 can be further simplified:

$$\beta = \frac{N\pi Z_0 k k_{10} l_1^6 e_0^4 e^{-2\alpha d} \sin^2\left(\frac{2\pi L}{\lambda_g}\right)}{9abRR_s(R+h)(K(e_0) - E(e_0))^2 \left(1 + \frac{Z_0 R}{2R_s(R+h)}\left(\frac{v_g}{c}\right)\right)} \left(\frac{\pi}{a\Gamma_{10}}\right)^2 \tag{36}$$

where R_s is the metal surface resistance. If the aperture is circular with radius r the attenuation coefficient should be expressed as $\alpha = \frac{2\pi}{\lambda}((\frac{\lambda}{3.41r})^2 - 1)^{1/2}$.

As an numerical example of a travelling wave structure with $h = 0.02$, $R = 0.04$, $v_g/c = 0.03$, $a = 0.072$, $b = h$, $\lambda = 0.1$, $N = 2$, $d = 0.0023$, $L = \lambda_g/4$, and $2l_2 = h$, one gets from eq. 36 that for $\beta = 1$ the coupling aperture's length $2l_1$ should be 0.037 which is very close to the HFSS simulation result [6].

3 Conclusions

In this paper we have shown in a general way how to establish the coupling coefficient between a waveguide and a cavity. This method can be used either for the fundamental mode or the higher order mode cases. As a special example we have established the analytical expression of the coupling coefficient for a system shown in Fig. 1.

References

[1] A.N. Parvenov, N.P. Sobenin, and B.V. Zverev, "Analytical calculation of a coupler for the linear collider accelerating section", EPAC94, p. 2022.

[2] S.V. Ivanov, et al., "DEAY linear collider accelerating section coupler", EPAC94, p. 2025.

[3] J. Gao, "Analytical formula for the coupling coefficient β of a cavity-waveguide coupling system", *Nucl. Instr. and Methods*, A309 (1991), p. 5.

[4] J. Gao, "Analytical Approach and scaling laws in the design of disk-loaded traveling wave accelerating structures", *Particle Accelerators*, Vol. 43(4) (1994), p. 235.

[5] R.E. Colling, "Field theory of guided waves", McGraw-Hill (1960).

[6] P. Avrakhov, "Simulation of TW buncher for CTF3", LAL/SERA internal report, Setp. 2000.

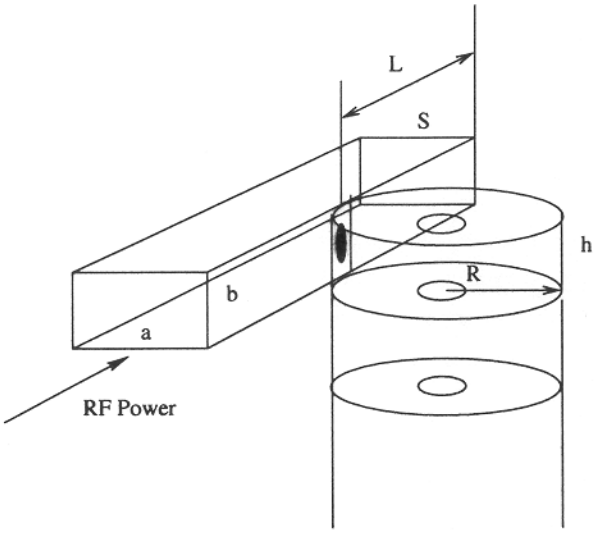

Figure 1: A waveguide cavity coupling system type I.

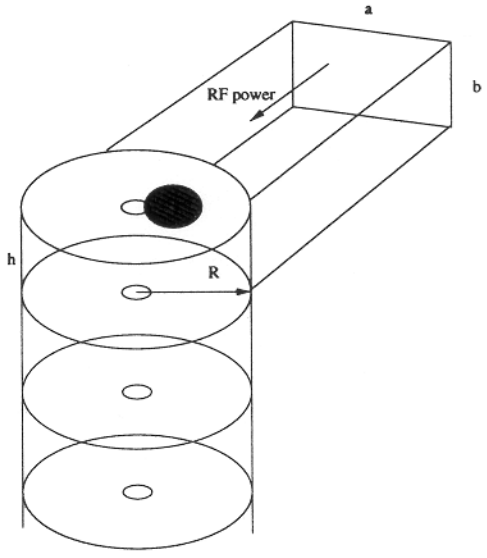

Figure 2: A waveguide cavity coupling system type II.

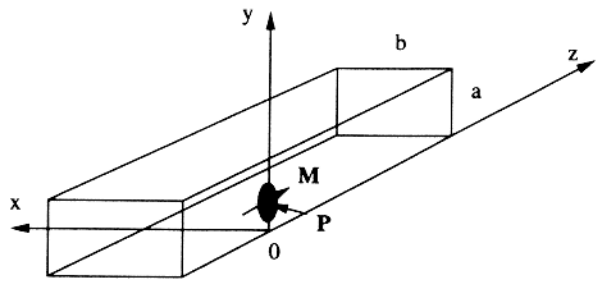

Figure 3: Waveguide excited by an electric dipole and a magnetic dipole.

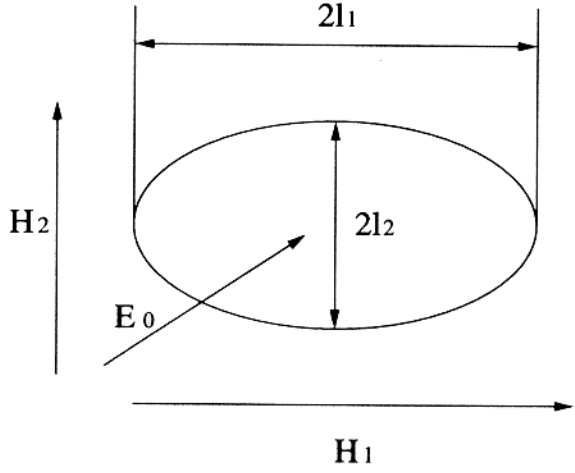

Figure 4: The elliptical coupling aperture with magnetic fields parallel to the surface and the electric field perpendicular to the surface.

Conclusions

- According to LAL-CTF3/CERN collabration program, a complete beam dynamics simulation for the CTF3 injector (initial phase) has been finished. For the two options (one and two prebunchers), the PARMELA simulation results show that they satisfy the required specifications.

- A preliminary design of the TW buncher has been started and is till going on.
- An analytical formula for the determination of the coupling coefficient of the waveguide-cavity coupling system used in the TW buncher and the fully beam-loaded accelerating structures has been established.

Acknowledgement

- We thank T. Garvey for his support to the LAL-CTF3/CERN collabration program.